296

Fragmentation patterns of selected ergot alkaloids by electrospray ionization tandem quadrupole mass spectrometry

Revised manuscript: 4-20-04

Andreas F. Lehner[1*], Morrie Craig[2], Neil Fannin[3], Lowell Bush[3], Thomas Tobin[1]

[1]University of Kentucky, Dept. of Veterinary Science, Maxwell H. Gluck Equine Research Center, Lexington, Kentucky, USA 40546

[2]Oregon State University, College of Veterinary Medicine, Corvallis, Oregon, USA 97331

[3]University of Kentucky, Dept. of Agronomy, Plant Science Building, Lexington, Kentucky, USA 40546

Running Title: ESI-MS/MS of ergot alkaloids

*Correspondence to:

Andreas F. Lehner, University of Kentucky, Dept. of Veterinary Science, Maxwell H. Gluck Equine Research Center, Lexington, Kentucky, USA 40546; Telephone: 859-257-4173; e-mail: alehner@uky.edu

Published as # 296 from the Equine Pharmacology, Therapeutics and Toxicology Program at the Maxwell H. Gluck Equine Research Center and Department of Veterinary Science, University of Kentucky and as Kentucky Agricultural Experiment Station Article # 02-14-60 with the approval of the Dean and Director, College of Agriculture and the Kentucky Agricultural Experimental Station. Supported by grants from the USDA Agriculture Research Service Specific Cooperative Agreement #58-6401-2-0025 for Forage-Animal Production Research, the Kentucky Department of Agriculture, the Kentucky Thoroughbred Association Foundation, the Horesemen's Benevolent and Protective Association, and Mrs. John Hay Whitney.

Submitted to *The Journal of Mass Spectrometry*

Tall fescue toxicosis and other maladies in livestock result from ingestion of vasoconstrictive ergot alkaloids produced by fungal endophytes associated symbiotically with the grass. In order to facilitate future analyses of grass extracts considered responsible for outbreak of related livestock diseases, we examined the electrospray ionization (ESI) mass spectra of specific ergot alkaloids under conditions that enable protonation. Our purposes were both to record the spectra with interpretation of mechanisms of fragmentation, as well as to derive commonalities that would enable prediction of mass spectra of related compounds for which standards were not readily available. With $[M+H]^+$ values in parentheses, water-insoluble lysergic acid peptide ergot derivatives ergovaline (m/z 534), ergotamine (m/z 582), ergocornine (m/z 562), ergocryptine (m/z 576) and ergocrystine (m/z 610) exhibited a consistent loss of water (-18 amu) from the C-12' alpha hydroxy functionality. Of this group, ergovaline and ergotamine generated an m/z 320 fragment deriving from cleavage of ring E amide and ether functions with retention of the peptide ring system methyl group. Ergocornine, ergocryptine and ergocrystine similarly formed an m/z 348 fragment with retention of isopropyl. These assignments were supported by the lack of similar fragments from the water-soluble ergot, ergonovine, which lacks a peptide ring system. Clavine-type ergot alkaloids lysergic acid and lysergol lack any substituents beyond simple ones directly on the C-8 position, and, similarly to ergonovine, lack significant fragments at m/z 268, 251 and 225 shared by the peptide ergot alkaloids.

Keywords: Ergot alkaloids; Tall Fescue Toxicosis; Mare Reproductive Loss Syndrome

Introduction

Tall fescue toxicosis in livestock appears to result from ingestion of grasses harboring a complex symbiotic relationship involving fungal endophyte habitation. The perennial grass *Festuca arundinacea*, or tall fescue, spreads via seed-propagation on over 35 million acres of pasture in the U.S.[1,2] Nutritionally it is considered one of the best forages for livestock including horses[3]. Since it is one of the most widely known forage grasses for horses, its toxic properties have recently been considered of possible significance in equine reproductive processes[4], as well as in the April-May 2001 outbreak of Mare Reproductive Loss Syndrome (MRLS) in Kentucky Bluegrass horse farms[5] (reports and updates on this syndrome available on the Internet[6]). This is of particular interest owing to previous studies describing vasoconstrictive and uterine-stimulating properties of certain endophyte alkaloids[1,4,7,8].

While it is known that different endophytic fungi infect different species of grasses and produce different arrays of toxins[8], one pharmacologically important group of indole alkaloids derived from seedhead-infecting fungi is the ergoline or ergot-type alkaloids; these are isolated from the dried sclerotium of the fungus *Claviceps purpurea,* a parasite on many grasses, rye, wheat and other grains[10]. There are three main groups of such ergot alkaloids, including the clavine group, the water-soluble lysergic acid type, and the water-insoluble lysergic acid type or peptide ergot alkaloids (see general structure, Fig. 1). These alkaloids are not especially useful pharmacologically, but agroclavine is a powerful uterine stimulant, and many of the ergot alkaloids are prolactin-release inhibitors. Ergonovine has potent uterine contraction activity and is used in treating postpartum hemorrhages. It also has significant vasoconstrictor activity[11].

There is a distinct need for understanding the fragmentation mechanisms of these classes of toxins as revealed by the relatively newer ionization methods of atmospheric pressure ionization (API) combined with mass spectrometry. The impetus for such research was the discovery of unknown endophyte-associated alkaloid peaks on HPLC chromatograms of clinical sample extracts involving suspected fescue toxicosis from Oregon State University's Diagnostic Laboratory in Oregon.

In order to identify new and possibly toxic ergopeptides and related unknown chromatographic peaks, characterization of known standards and their metabolic products was essential. Several standards of ergot alkaloids were examined, including clavine-type (lysergic acid, lysergol), water-soluble lysergic acid derivatives (ergonovine) and water-insoluble lysergic acid peptide derivatives (ergotamine, ergocornine, ergocryptine, ergovaline, ergocrystine) for patterns of electrospray(+) ionization-mass spectrometric [ESI(+)MS] fragmentation. The resultant understanding of fragmentation events facilitated HPLC-MS/MS examination of methanol extracts of grasses for ergot alkaloids, as will be reported separately. This work builds on earlier work by Yates, et al.[12] who carried out similar analytical method development, but used isobutane negative ion chemical ionization (NICI) of thermally desorbed and partially-fragmented compounds, and on work of Shelby and Flieger who developed gradient-HPLC-fluorescence methods with LC-MS identification of over 10 ergots following epimerization[13]. The soft ionization techniques of electrospray utilized in our current approach provide the advantage of avoiding the preliminary fragmentation of NICI-MS in data reported here. Chromatographic work extending that of Shelby and Flieger will be reported in a future article.

Experimental

Compounds

Ergovaline was isolated from tall fescue as previously described[14]. Its concentration was estimated spectrophotometrically and diluted to 1.0 ug/ml in methanol. Other ergot alkaloids were obtained from Sigma. Ergonovine, ergotamine tartrate, ergocryptine, ergocrystine, lysergic acid and lysergol standards were prepared as 1.00 μg/ml stocks of parent compound in methanol. Ergocornine was prepared similarly but was more readily soluble in ethyl acetate than in methanol.

Electrospray ionization (ESI) mass spectrometry

Ergot alkaloid standards or extracts were prepared for direct infusion ESI (positive mode) MS analysis by dilution 1:5 or 1:10 with 0.05% formic acid (aq):acetonitrile, 1:1. Infusion was carried out with a Harvard syringe pump equipped with a 500 ul Hamilton gastight syringe with infusion at 1.0 ml/hr. The mass spectrometer is a Micromass (Beverly, MA) Quattro II ESI-MS/MS, and typical ESI-MS voltage settings for detection and analysis of various ergots were as follows: capillary, 3.15 kV; HV lens, 0.5 kV; cone, 30 V; skimmer lens, 1.0 V; RF lens, 0.1 V; source temperature, 120° C.; argon pressure for collisionally-induced dissociation (CID) experiments, 3-4 x 10^{-3} mbar; ionization energies: MS1, 0.5 V; MS2, 13.0 V. Collision energy was set between 24 and 32 eV. ESI-MS and MS/MS spectra were acquired as continuum data for a minimum of 1-2 min. over the m/z 10-800 mass range, applying 1.8 seconds per scan duration. Resultant data were background subtracted and smoothed with the Micromass MassLynx version 3.4 software. Spectra were deconvoluted with the assistance of Mass Spec Calculator Pro software, version 4.03 (Quadtech Associates, Inc., 1998). Where appropriate, optimized semi-empirical three-dimensional structures were computed by application of an AM1 subprogram of HyperChem, Release 3 (Autodesk, Inc., 1993). Mass spectral fragmentation schemes were derived with reference to McLafferty and Turecek[15].

Results

Ergovaline

Ergovaline combines a methyl group on its 5-member lactam ring E with an isopropyl group on its peptide ring system central F ring (ring designations in Fig. 1). Fig. 2 shows the ergovaline MS and daughter ion spectra (A and B, respectively), with interpretations of daughter ion fragments in the figure legend. Cleavages to release the m/z 223 fragment and its demethylated counterpart at m/z 208 are illustrated as a Fig. 2 insert. Cleavage at the carbonyl group of the amide functionality is expected to generate an even-electron cation, designated EE^+, at m/z 223[15]; therefore, assuming a two-stage fragmentation, loss of CH_3 to generate m/z 208 must proceed by elimination of $CH_3^\bullet$ as a radical and would thus represent a violation of the even-electron rule[16], although many exceptions to this rule are known to exist[16-19]. This rule can be simply summarized as

$EE^+ \rightarrow EE^0$ [neutral] + EE^+ fragmentations are normally greatly favored over

$EE^+ \rightarrow OE^\bullet + OE^{\bullet+}$, where OE represents an odd-electron species

The apparent m/z 223→208 process became a recurring fragmentation motif with these compounds, and is examined with the next compound ergotamine in greater detail.

Figure 2C expands measured intensities in the vicinity of the [M+H] pseudomolecular ion of ergovaline, m/z 534.4, with intensity values for [M+1+H] at 535.4, and [M+2+H] at 536.4 of 34.3% and 6.0%, respectively, relative to [M+H]. These correspond well to those calculated by Mass Spec Calculator software for a $C_{29}H_{36}N_5O_5$ compound, as illustrated in Fig. 2D. Note the significant m/z 270 peak found in the ESI(+)MS scan in Fig. 2A, which was found to be a recurring contaminant in other preparations.

Ergotamine

Ergotamine combines a methyl group on its 5-member lactam ring with a benzyl group on its peptide ring system central ring. As seen with ergovaline in Fig. 2B, the recurring tertiary alcohol again favored CID-induced dehydration, and the ergotamine ESI-MS and daughter ion spectra are

shown in Fig. 3A and B. Ergotamine [M+H], [M+1+H] and [M+2+H] intensities were observed as 100%, 39.8% and 8.8% respectively, which compared well to values of 100%, 39.3% and 8.4% for a $C_{33}H_{36}N_5O_5$ compound. Cleavages to release the m/z 223 fragment and its demethylated counterpart at m/z 208 are illustrated as a Fig. 3 insert. The figure legend lists peak assignments for the major ergotamine daughter ion fragments.

As mentioned in the section on ergovaline, generation of m/z 223 and 208 by two-step fragmentation would involve processes summarized as $EE^+ \rightarrow OE^\bullet + OE^{\bullet+}$, generally considered to be disallowed owing to the requirement for electron pair separation. Since, as will be seen, these fragments occurred in all the ergots examined, except lysergol, we examined this phenomenon in greater depth. Fig. 4A displays a selected m/z 200-280 range of an ergotamine ESI(+)MS spectrum run as in Fig. 3 except with a high cone voltage of 50V intended to induce in-source fragmentation; both m/z 223 and 208 became visible under these conditions. Fig. 4B demonstrates that [M+H] daughter ions of m/z 582 were generally similar in pattern to those obtained in Fig. 3B under these conditions. Fig. 4C shows that daughter ion analysis of the in-source generated m/z 223 fragment included m/z 208 among its progeny ions, demonstrating that this fragmentation is in fact an exception to the even-electron rule. However, the m/z 208 fragment was somewhat obscured by a significant m/z 207 as part of a cluster of ions from m/z 205-208. Therefore, a parent ion scan for the m/z 208 product was included (Fig. 4D), which more clearly demonstrated its origin from m/z 223, as well as from 225, 251, 268 and 277, all ions likely to include the lysergic acid ring system (rings A-D in Fig. 1). The results of Fig. 4 were not peculiar to ergotamine, as nearly identical results were obtained from ergocryptine [not shown].

Ergocornine

Ergocornine (ESI(+)MS in Fig. 5A) is the first of three compounds with an isopropyl group on its 5-member lactam E ring; it also includes an isopropyl group on its peptide ring system central ring. Ergocornine [M+H], [M+1+H] and [M+2+H] intensities were observed as 100%, 34.5% and 5.0% respectively, which compared relatively well to values of 100%, 37.1% and 7.6% for a $C_{29}H_{36}N_5O_5$ compound. This compound was capable of undergoing dehydration to a m/z 544.2 derivative, which

was in turn responsible for several of the principal daughter ion fragments, in particular 305, 277, 261 and 195 (Fig. 5B). Cleavages to release the m/z 223 fragment and its demethylated counterpart at m/z 208 are illustrated as a Fig. 5 insert. The figure legend summarizes fragment descriptions or cleavage events giving rise to each principal ion.

Ergocryptine

Ergocryptine differs from ergocornine only in the presence of an additional side chain methylene group converting an isopropyl to an isobutyl group. It underwent dehydration as well, and yielded other peaks similar to those of ergocornine (MS and daughter ion spectra are shown in Fig. 6, A and B, respectively). [M+H], [M+1+H] and [M+2+H] intensities were observed as 100%, 36.0% and 8.0% respectively, which compared well to calculated values of 100%, 38.3% and 8.0% for a $C_{32}H_{42}N_5O_5$ compound. Cleavages to release the m/z 223 fragment and its demethylated counterpart at m/z 208 are illustrated as a Fig. 6 insert. Differences in peak relative intensities from those of ergocornine may be a consequence of slight differences in tuning parameters. Peak assignments for principal peaks are listed in the figure legend.

Ergocrystine

Ergocrystine has the benzyl group of ergotamine, but also contains the isopropyl group on its 5-member lactam E ring as seen in ergocornine and ergocryptine. It underwent dehydration as well, and yielded other peaks similar to those of ergocornine. Fig. 7 shows the ergocrystine MS and daughter ion spectra (A and B, respectively), with interpretations of daughter ion fragments listed in the figure legend. [M+H], [M+1+H] and [M+2+H] intensities were observed as 100%, 40.3% and 9.7% respectively, which compares well to values of 100%, 41.6% and 9.3% calculated for a $C_{35}H_{40}N_5O_5$ compound. Cleavages to release the m/z 223 fragment and its demethylated counterpart at m/z 208 are illustrated as a Fig. 7 insert.

Ergonovine

Ergonovine (ESI(+)MS in Fig. 8A, daughter ion spectrum in 8B) showed a pattern of m/z 223 and 208 daughter ion fragments similar to those in ergovaline, ergotamine, ergocornine, ergocryptine and ergocrystine, which confirms structural assignments for these fragments since ergonovine lacks the peptide ring system and must therefore derive m/z 223 and 208 from the lysergic ring system held in common. Likewise, the previous ergots displayed dehydration peaks generally in both ESI(+)MS scans and daughter ion spectra, which phenomenon was absent from ergonovine and which supported the peptide ring system origin from the tertiary alcohol group. The other main fragment at m/z 180 on daughter ion analysis (Fig. 8B), was one of several fragments arising in turn from the initial cleavage at the carbonyl group to release a 223 amu-sized fragment (initial cleavage to m/z 223 shown in figure insert, along with m/z 208). Peak assignments for principal peaks are listed in the figure legend. Many of the peaks identified turned out to be a recurrent pattern with the ergot alkaloids family, as will be discussed later. [M+H], [M+1+H] and [M+2+H] intensities were observed as 100%, 21.7% and 2.6% respectively, which compares well to values of 100%, 22.7% and 2.7% for a $C_{19}H_{24}N_3O_2$ compound.

Lysergol

Lysergol represents the reduced alcohol form of the lysergic acid-type clavine alkaloid. Fig. 9 shows the lysergol MS and daughter ion spectra (A and B, respectively), with interpretations of daughter ion fragments listed in the figure legend. Cleavage to release the m/z 224 fragment and the demethylated m/z 240 are illustrated in the figure insert. [M+H], [M+1+H] and [M+2+H] intensities were observed as 100%, 20.5% and 2.3% respectively, which compared well to values of 100%, 18.9% and 1.8% for a $C_{16}H_{19}N_2O_1$ compound.

Lysergic acid

Lysergic acid represents the immediate synthetic precursor of the pharmacologically important natural ergot alkaloids, via amide linkage to the position-8 carboxy group. Fig. 10 shows the lysergic acid ESI(+)MS and daughter ion spectra (A and B, respectively), with interpretations of daughter ion fragments listed in the figure legend. Note that intense dissociation of $CH_2{=}NHCH_3^+$ by cleavage of the D-ring affected the appearance of the rest of the spectrum, generally suppressing relative ion intensity of other fragmentation events. As an example, cleavage of the D-ring to release the m/z 167 fragment is illustrated in the figure insert. The m/z 44 ion was present throughout the surveyed compounds, but was more intense in lysergol and lysergic acid under these conditions, and possibly indicated a stabilizing influence of the amide function. [M+H], [M+1+H] and [M+2+H] intensities were observed as 100%, 18.2% and 2.9% respectively, which compared well to values of 100%, 18.9% and 2.0% calculated for a $C_{16}H_{17}N_2O_2$ compound.

Ergot alkaloid breakdown products

Certain ergot alkaloid preparations showed evidence consistent with the presence of contaminants arising presumably by hydrolysis or oxidation of the principal intact component, or perhaps by incomplete purification of a synthetic or natural product. The most significant such contaminant occurred consistently at m/z 270 (daughter ion spectrum shown in Fig. 11), which as an [M+H] singly charged species indicated an uncharged compound molecular weight of 269. This odd m.w. most likely indicated an odd number of N atoms, and since this species was seen with equivalent mass spectra in ergovaline, ergocryptine and lysergol, it most likely indicated a lysergic ring species with an additional nitrogen-containing functionality. The Fig. 11 insert offers a suggested structure, as a reduced form of lysergic acid amide. The figure legend lists assignments of major peaks seen in the Fig. 11 daughter ion spectrum in keeping with the general possibility of a lysergic acid ring system-derived structure. [M+H], [M+1+H] and [M+2+H] intensities were observed in the lysergol prep 269 m.w. compound as 100%, 19.7% and 1.6% respectively, which would seem to confirm the structure shown, or at least its molecular formula, which predicted values of 100%, 19.3% and 1.8% for a $C_{16}H_{20}N_3O_1$ compound.

Discussion

This survey of principal ergot alkaloid compounds by ESI(+)-MS and MS/MS has enabled assignment of fragments by comparisons of compounds with one another, and in turn revealed commonalities of fragmentation events. Table 1 lists ion fragments found in common in the ergot alkaloid standards. This data set reveals that valine-derived ergopeptides (those with R_1=isopropyl in Fig. 1) display m/z 348, whereas alanine-derived ergopeptides (those with R_1=methyl in Fig. 1) display m/z 320. This assignment is supported by the absence of either peak in ergonovine, lysergol or lysergic acid, all three of which lack the peptide ring systems. A potential generic fragmentation mechanism is displayed in Fig. 12, displayed here to account for major fragments of ergocornine ($[M+H]^+$, m/z 562) as an example. Cleavage to release the protonated lysergic ring system including the central amide linkage accounts for m/z 268. Otherwise, dehydration at the peptide tertiary alcohol occurs with intramolecular proton transfer from the lysergic D ring tertiary amine or C-7 with generation of a tertiary carbonium ion at C-12' to account for m/z 544. Cleavage of the m/z 544 D ring with loss of the R_2 group accounts for m/z 305 [common only to R_1 = isopropyl compounds per Table 1]. Alternatively, cleavage to release the entire lysergic ring system including the central amide linkage accounts for m/z 277. The m/z 544 dehydrate can undergo charge migration with concerted electron transfers to give a structure capable of cleavage to the major peak m/z 348 or the minor fragment m/z 195. This survey has accounted for ergocornine m/z 562, 544, 348, 305, 277, 268 and 195 ions by mechanisms directly applicable to the other compounds examined; m/z 223 and 208 are the other major ions generated as shown schematically in Figs. 2-3 and 5-8, with m/z 208 apparently arising by violation of the even-electron rule as demonstrated in Fig. 4.

The positing of an intramolecular proton shift for generation of a carbonium ion during dehydration was suggested above to account for the difficulty that simple direct scission of the 5-member lactam ring E yields a fragment 2 amu greater than required in the case of each ergotoxin. Molecular modeling with Hyperchem software was performed to provide a geometry-optimized three-dimensional structure for ergocornine as an example, and this revealed that the C-7 alpha proton and the hydroxyl group oxygen atom are relatively sequestered and only 1.831 Å apart, making such a

transfer highly plausible (structures shown in Fig. 13). This contrasts with crystallographic findings from studies of dehydrated crystals, which suggest rigid central amide O to C-12' OH hydrogen bonding as a general ergopeptide motif[20]; however, the new proposed arrangement requires simple rotation of the C-2' carbon-nitrogen bond to depart from the hydrogen bonding arrangement suggested by the x-ray structure. Further rotation around the bond from C-8 to the amide carbonyl group can also bring the C-12' hydroxyl oxygen atom and D-ring amine nitrogen atom within 2-3 Å, implying that ammonium proton transfer to C-12' OH is likely to be at least an equivalent possibility.

The m/z 223 fragment observed and illustrated in Figs. 2-3 and 5-8 requires cleavage at the C-8 carbon atom, and a potential fragmentation pathway is suggested in Fig. 14. Molecular modeling indicated proximity of the carbonyl oxygen and quarternary amine proton only following epimerization at C-8 (data not shown).

With regard to other common fragments in Table 1, strong m/z 277 fragments from ergovaline and ergocornine, as well as m/z 291 from ergocryptine, seemed to correlate well with loss of R_1 and the lysergic ring system from corresponding dehydrates; this transition wasn't found for the R_2 = benzyl compounds. There is apparently an alternative structure for m/z 277 that includes the lysergic ring system, since minor m/z 277 peaks were seen from ergotamine and ergocrystine, and m/z 277 was seen as a parent to m/z 208 in ergocornine (Fig. 4) and ergocryptine. The m/z 225 fragment was originally considered as deriving from the peptide ring system owing to its presence only in the spectra of peptide-ring system-containing compounds, and conversely its absence in ergonovine, lysergol and lysergic acid. However, its occurrence as a parent ion for m/z 208 (Fig. 4) implies inclusion of the lysergic ring system, with the simplest interpretation being a $+H_2$ variant of m/z 223 whose origin depends mechanistically upon the peptide ring system, particularly since ergonovine lacks both peptide ring system and m/z 225. The m/z 197 fragment can be accounted for by cleavage and release of a CH≡CH neutral fragment from m/z 223 simply from the D ring. The m/z 44 peak is of relatively minor intensity in most of the standards, and has been assigned a $CH_2{=}NHCH_3^+$ fragment arising from the D-ring. This fragment therefore unites the peptide-ring bearing ergotoxins with ergonovine and the clavine-type ergots, especially lysergol and lysergic acid where the m/z 44

fragment is of significant intensity (Fig. 10). The lack of m/z 44 from the 269 m.w. species probably speaks to its structure, most likely electronic configuration of the D-ring. The m/z 70 fragment is found only in those compounds with the peptide ring system, supporting its assignment as arising from two cleavages at an amide and a C-C bond to release a pyrrole ring. One curious finding concerned the differences in scission events between lysergol and lysergic acid, presumably guided by the differing oxidation states of the side chain: the series of fragments m/z 223, 208, 180 and 167, seen in lysergic acid and most likely having the same resultant structures as those in the other alkaloids, becomes m/z 224, 209, 180 and 168 in lysergol accounting for the absence of most of these peaks in its list of common fragments, Table 1.

The understanding of ergot alkaloid fragmentation as summarized in Table 1 enables predictions to be applied to compounds with closely related structures. Table 2 summarizes primary cleavages anticipated for a series of peptide- and non-peptide type ergot alkaloids seen in nature and related to and including those examined here. Although other fragments could also be included, this list focuses on those arising from loss of the peptide side chain and its associated NH_2-HC=O linkage as described in Figs. 2-3 and 5-9, along with the corresponding loss of methyl (minus 15) from the resulting fragment. This list could provide the basis for Multiple Reaction Monitoring (MRM) detectability in any tandem quadrupole instrument equipped with an electrospray inlet, whether the aim is quantitation of knowns such as the standards examined here, or detection of new compounds including those in Table 2. Application of these approaches to MRM detection of naturally-occurring ergot alkaloids will be reported in a forthcoming paper.

References

1. Putnam M., Bransby D., Schumacher J., Boosinger T., Bush L., Shelby R., Vaughan J., Ball D., Brendemuehl J. Effects of the fungal endophyte *Acremonium coenophialum* in fescue on pregnant mares and foal viability. *Am J Vet Res,* 1991; **12**:2071-2074.

2. Ball, D.M., Hoveland, C.S., Lacefield, G.D. "Southern Forages." Atlanta: The Potash and Phosphate Institute, 1991; p. 169ff .

3. Ball, D.M., Hoveland, C.S., Lacefield, G.D. "Southern Forages." Atlanta: The Potash and Phosphate Institute, 1991; p. 41 and 133.

4. Cross, D. Fescue toxicosis in horses. In: "Neotyphodium/Grass Interactions", Bacon, C.W., Hill, N.S., eds. New York: Plenum Press, 1997; pp. 289-309.

5. Schultz, C.L. and Bush, L.P. The potential role of ergot alkaloids in Mare Reproductive Loss Syndrome. In: "Proceedings of the First Workshop on Mare Reproductive Loss Syndrome", Powell, D.G., Troppmann, A., Tobin, T., eds. Lexington, Kentucky: Kentucky Agricultural Experiment Station, 2002; pp. 60-63.

6. University of Kentucky, College of Agriculture, Gluck Equine Research Center updates on MRLS: www.uky.edu/Ag/VetScience/mrls/index.htm

7. Abney, L.K., Oliver, J.W., Reinemeyer, C.R. Vasoconstrictive effects of tall fescue alkaloids on equine vasculature. *J. Equine Veter. Science,* 1993; **13**:334-340.

8. Redmond, L.M., Cross, D.L., Gimenez, T., Hudson, L.W., Earle, W.F., Kennedy, S.W. The effect of phenothiazine and withdrawal time on gravid mares grazing endophyte-infected tall fescue. *J. Equine Veter. Science,* 1991; **11**:17-22.

9. Aldrich-Markham S., Pirelli G. Endophyte Toxins in Grass Seed Fields and Straw. Corvallis, Oregon: Oregon State University Extension Service, Publication EM 8598, June 1995.

10. Mycotoxicoses. In: The Merck Veterinary Manual, Seventh Edition. C.M. Fraser, editor. Rahway, N.J.: Merck and Co., Inc. 1991; pp. 1678-1681.

11. Rall, T.W., Schleifer, L.S. Oxytocin, Prostaglandins, Ergot Alkaloids, and other drugs: Tocolytic agents. In: "Goodman and Gilman's The Pharmacological Basis of Therapeutics", Seventh Edition, Gilman, A.G., Goodman, L.S., Rall, T.W. , Murad, F., eds. New York: Macmillan Publishing Co., 1985; pp. 926-945.

12. Yates, S., Plattner, R., Garner, G. Detection of Ergopeptine Alkaloids in Endophyte Infected, Toxic Ky-31 Tall Fescue by Mass Spectrometry/Mass Spectrometry. *J. Agric. Food Chem.,* 1995; **33**:719-722.

13. Shelby, R.A., Flieger, M. Analysis of ergot alkaloids in plants and seeds of endophyte-infected tall fescue by gradient HPLC. In: "Neotyphodium/Grass Interactions", Bacon, C.W., Hill, N.S., eds. New York: Plenum Press, 1997; pp. 271-273.

14. Craig, A.M., Bilich, D., Hovermale, J.T., Welt, R.E. Improved extraction and HPLC methods for ergovaline from plant material and rumen fluid. *J. Vet. Diagn. Invest.,* 1994; **6**:348-352.

15. McLafferty, F.W., Turecek, F. "Interpretation of Mass Spectra. Fourth Edition." Sausalito, California: University Science Books, 1993.

16. Karni, M., Mandelbaum, A. The 'Even-Electron' Rule. *Organic Mass Spec.*, 1980; **15**:53-64.

17. Brown, R.D., Harrison, A.G. Loss of methyl radical from some small immonium ions: unusual violation of the even-electron rule. *Organic Mass Spec.*, 1981; **16**:180-182.

18. Krauss, D., Mainx, H.G., Tauscher, B., Bischof, P. Fragmentation of trimethylsilyl derivatives of 2-alkoxyphenols: a further violation of the 'Even-Electron Rule'. *Organic Mass Spec.*, 1985; **20**:614-618.

19. Ceraulo, L., Agozzino, P., Ferrugia, M., Lamartina, L., Natoli, M.C. Studies in organic mass spectrometry. Part 9-Mass spectra of 9,10-disubstituted 2,3,6,7-tetraalkoxy-9,10-dihydroanthracenes: a remarkable loss of radicals from even-electron ions. *Organic Mass Spec.*, 1991; **26**:279-286.

20. Petrícková, H., Husák, M., Jegorov, A. Conformation study of proline ring G in structures of ergopeptines. *Materials Structure*, 2001; **8**:60-61.

Figures

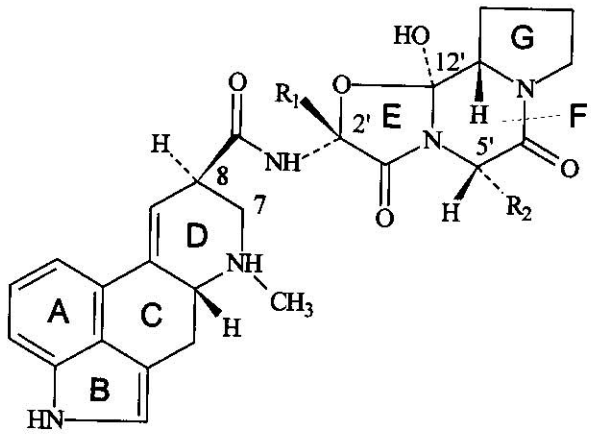

Fig. 1. General structure of peptide ergot alkaloids indicating stereochemistry and important numeric labels of positions and alphabetical labeling of rings. Where R_1 = methyl, R_2 is the following in respective compounds: isopropyl (ergovaline); benzyl (ergotamine). Where R_1 = isopropyl, R_2 is the following in respective compounds: isopropyl (ergocornine); isobutyl (ergocryptine); benzyl (ergocrystine). Structure and labels after Rall and Schleifer[11] and Petrícková, et al.[20].

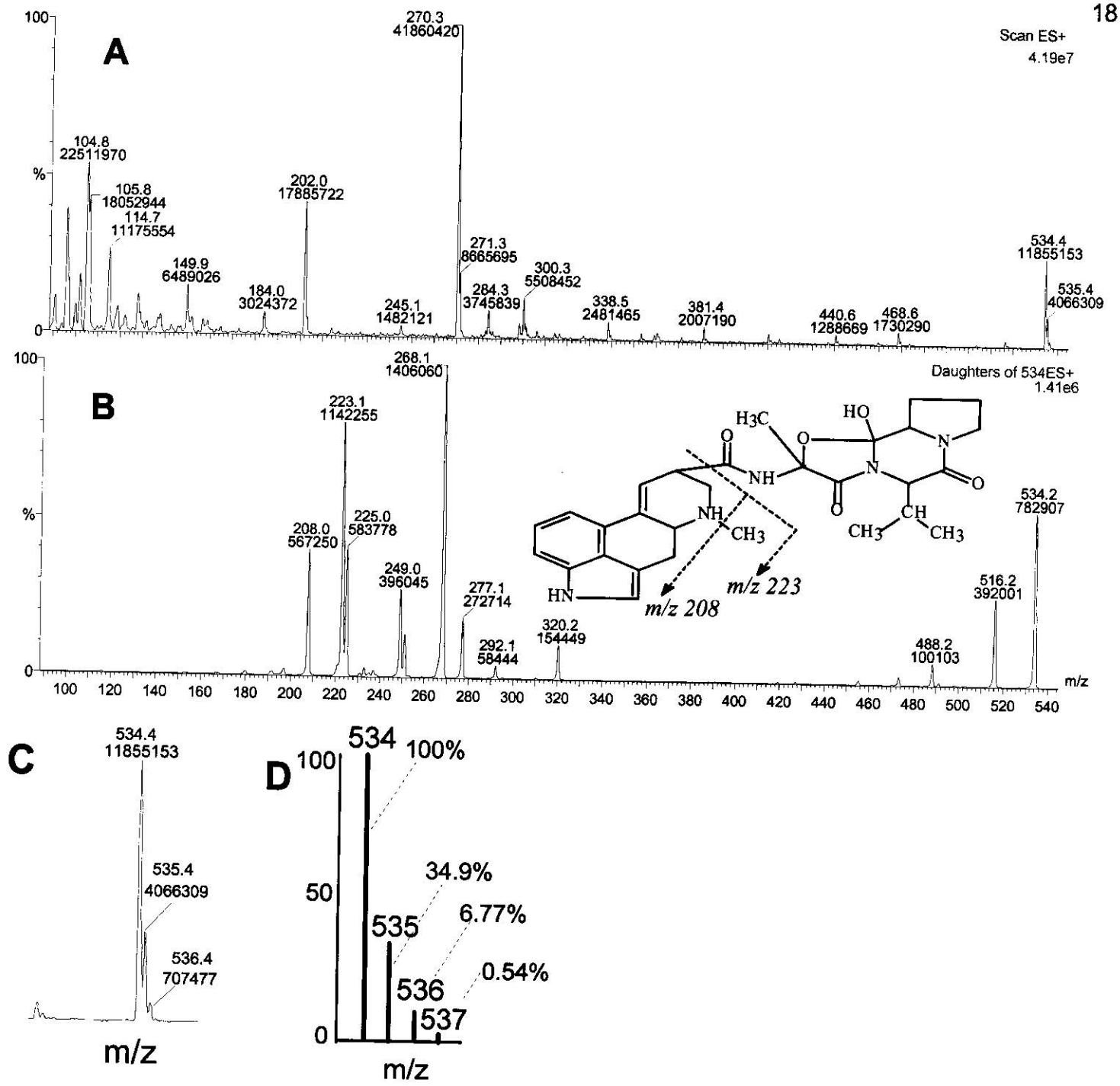

Fig. 2. [Legend next page]

Fig. 2. Ergovaline mass spectrometry. **A**, ESI(+) MS of ergovaline standard infused as a 0.2 ug/ml solution in acetonitrile:0.05% formic acid at 1.0 ml/hr into the Quattro II MS. **B**, daughter ion spectrum of the m/z 534.5 fragment seen in **A**. Daughter ion principal peak assignments: m/z 534, $[M+H]^+$; 516, loss of water (-18) from peptide ring system; 488, m/z 516 minus CO; 320, cleavage of peptide ring system (in amide and at ether); 292, m/z 516 minus lysergic ring system; 277, m/z 292 minus CH_3; 268, [lysergic ring system-C=O-NH_2] + H; 249, m/z 516 minus [lysergic ring system-C=O-NH_2]; 225, likely $+H_2$ variant of m/z 223; 223, $[M+H]^+$ minus [peptide side chain-NH-HC=O]; 208, m/z 223 minus CH_3; 197, m/z 223 minus CH≡CH; 180, 223 minus CH_2=NCH_3; 70, pyrrole ring + H; 44, CH_2=$NHCH_3$. The insert shows ergovaline structure protonated on the lysergic ring tertiary amine and indicating collisionally-induced dissociation with the origins of the m/z 223 and 208 fragments. Peak labels in this and subsequent spectra show measured m/z value [upper value] and measured intensity [lower value]. **C**, Measured intensities in the vicinity of the $[M+H]^+$ molecular ion; **D**, calculated intensities (MS Calculator Pro).

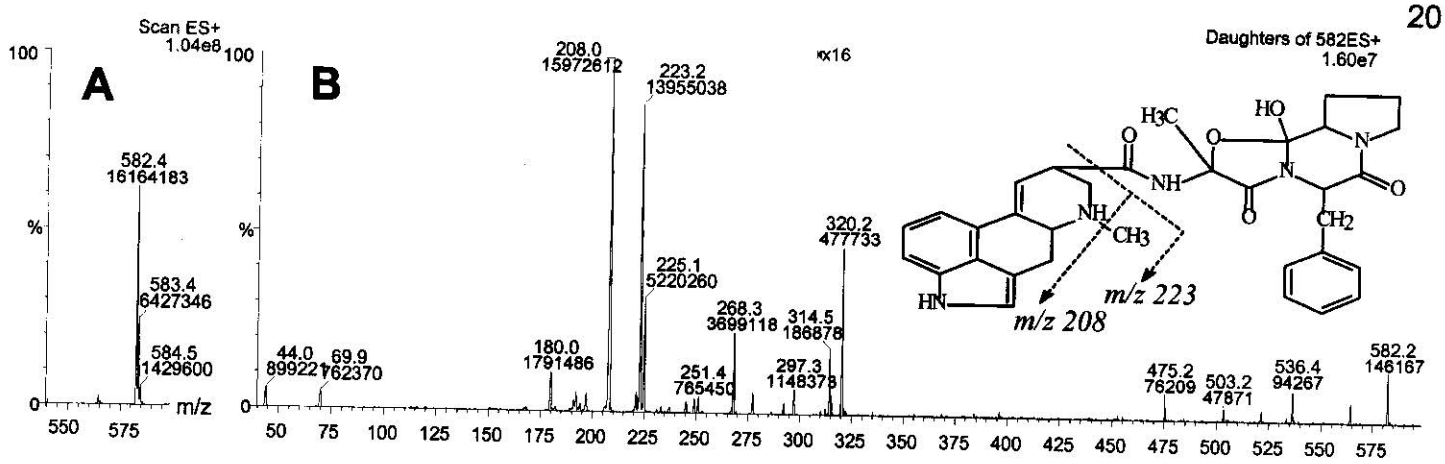

Fig. 3. Ergotamine mass spectrometry. **A**, ESI(+) MS of ergotamine infused as a 0.2 ug/ml solution in acetonitrile:0.05% formic acid at 1.0 ml/hr into the Quattro II MS. **B**, daughter ion spectrum of the m/z 582.4 fragment seen in **A**; note the 16-fold enhancement of fragment intensities above m/z 310. Daughter ion principal peak assignments: m/z 582, $[M+H]^+$; 564, loss of water (-18) from peptide ring system; 536, m/z 564 minus CO; 503, $[M+H]^+$ minus C_6H_5 with transfer of a proton; 475, $[M+H]^+$ minus CH_3 and $CH_2C_6H_5$ groups with transfer of a proton; 320, cleavage of peptide ring system (in amide and at ether); 297, 564 minus [lysergic ring system-$CONH_2$]; 268, [lysergic ring system-C=O-NH_2] + H; 225, likely +H_2 variant of m/z 223; 223, $[M+H]^+$ minus [peptide side chain-NH-HC=O]; 208, m/z 223 minus CH_3; 197, m/z 223 minus CH≡CH; 180, m/z 223 minus CH_2=NCH_3; 70, pyrrole ring + H; 44, CH_2=$NHCH_3$. The insert shows ergotamine structure protonated on the lysergic ring tertiary amine and indicating collisionally-induced dissociation with the origins of the m/z 223 and 208 fragments.

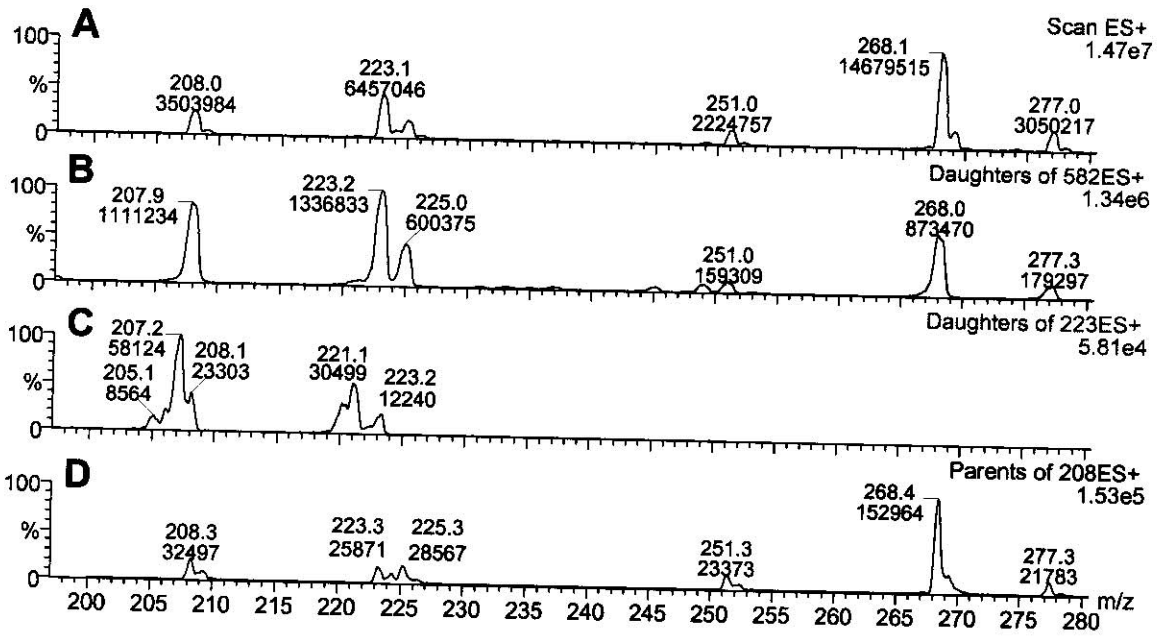

Fig. 4. Relevant spectra demonstrating violation of the even-electron rule in ergotamine. 10 ug/ml ergotamine tartrate in 0.5% formic acid:acetonitrile 1:1, was infused into the Quattro II ESI(+)MS at 1.2 ml/h, with the relatively high cone voltage setting of 50 V; collision energy was 24 eV where appropriate. Scans from top to bottom include: A, full scan; B, m/z 582 daughter ion scan; C, m/z 223 daughter ion scan and; D, m/z 208 parent ion scan. ACD/MS Fragmenter software, version 1.01 (2003; ACD Labs, Toronto, Canada) indicates likely origins for the m/z 223 fragments in Fig. 4C as m/z 221, loss of H_2; 208, loss of $CH_3^{\bullet}$; 207, loss of CH_4; 206, loss of NH_3; 220 would involve unusual loss of $H_3^{\bullet}$, from which loss of $CH_3^{\bullet}$ would then account for 205.

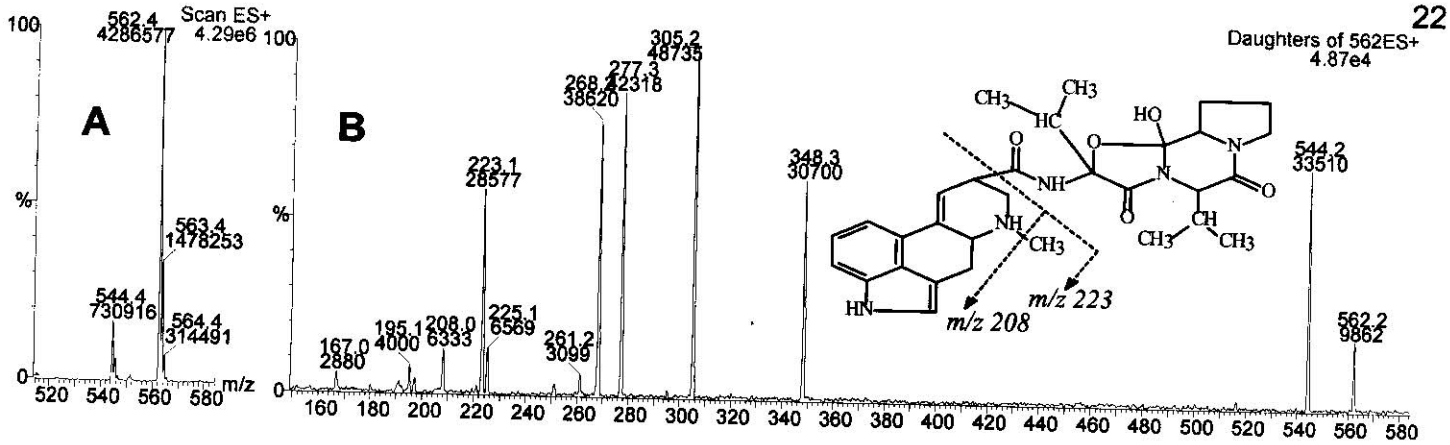

Fig. 5. Ergocornine mass spectrometry. **A**, ESI(+) MS of ergocornine infused as a 0.2 ug/ml solution in acetonitrile:0.05% formic acid at 1.0 ml/hr into the Quattro II MS. **B**, daughter ion spectrum of the m/z 562 fragment seen in **A**. Daughter ion principal peak assignments: m/z 562, $[M+H]^+$; 544, loss of water (-18) within peptide ring system; 516 [minor], 544 minus CO; 348, cleavage within and loss of most of peptide ring system (in amide and at ether); 305, m/z 544 minus R_2 group plus cleavage of lysergic D ring to retain first 2 carbons; 277, m/z 544 minus [lysergic ring system-$CONH_2$]; 268, [lysergic ring system-C=O-NH_2] + H; 225, likely +H_2 variant of m/z 223; 223, $[M+H]^+$ minus [peptide side chain-NH-HC=O]; 208, m/z 223 minus CH_3; 197, m/z 223 minus CH≡CH; 180, m/z 223 minus CH_2=NCH_3; 167, m/z 223 minus CH_2=$CHNCH_3$; 70, peptide ring system pyrrole [C_4H_8N]; 44, CH_2=$NHCH_3$. The insert shows ergocornine structure protonated on the lysergic ring tertiary amine and indicating collisionally-induced dissociation with the origins of the m/z 223 and 208 fragments.

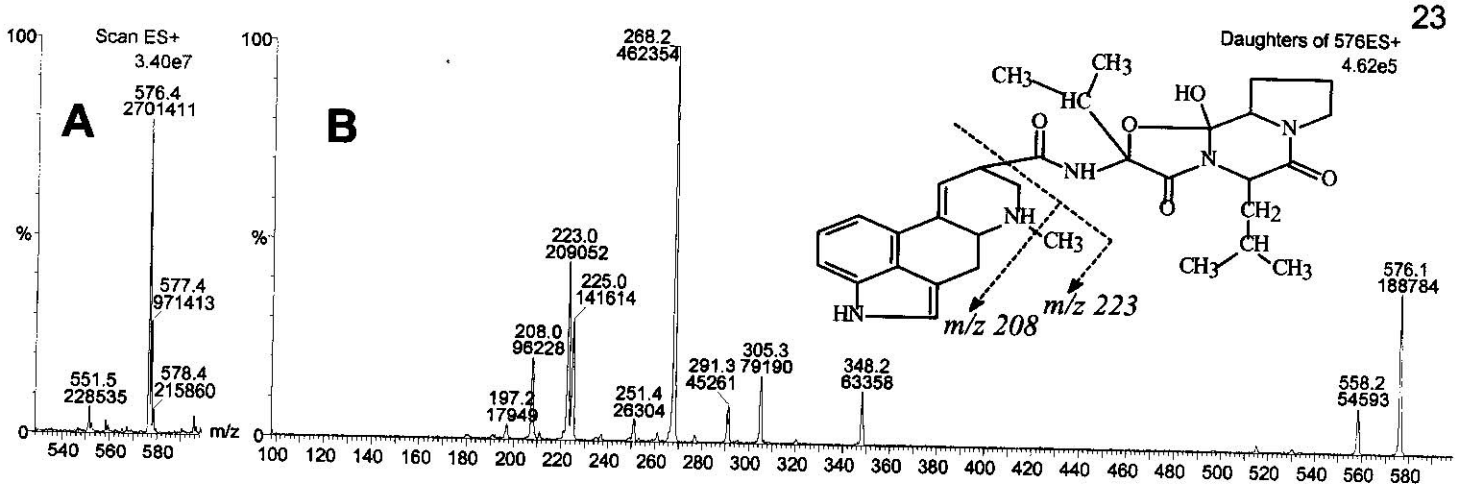

Fig 6. Ergocryptine mass spectrometry.**A**, ESI(+) MS of alpha-ergocryptine infused as a 0.2 ug/ml solution in acetonitrile:0.05% formic acid at 1.0 ml/hr into the Quattro II MS. **B**, daughter ion spectrum of the m/z 576.5 fragment seen in **A**. Daughter ion principal peak assignments: m/z 576, $[M+H]^+$; 558, loss of water (-18) from peptide ring system; 530 [minor], 558 minus CO; 348, cleavage within and loss of peptide ring system (in amide and at ether); 305, m/z 558 minus R_2 group plus cleavage of lysergic D ring to retain first 2 carbons; 291, m/z 558 minus [lysergic ring system-C=O-NH_2]; 268, [lysergic ring system-C=O-NH_2] + H; 225, likely +H_2 variant of m/z 223; 223, $[M+H]^+$ minus [peptide side chain-NH_2-HC=O]; 208, m/z 223 minus CH_3; 197, m/z 223 minus CH≡CH; 180, m/z 223 minus CH_2=NCH_3; 70, pyrrole ring + H; 44, CH_2=$NHCH_3$. The insert shows ergocryptine structure protonated on the lysergic ring tertiary amine and indicating collisionally-induced dissociation with the origins of the m/z 223 and 208 fragments.

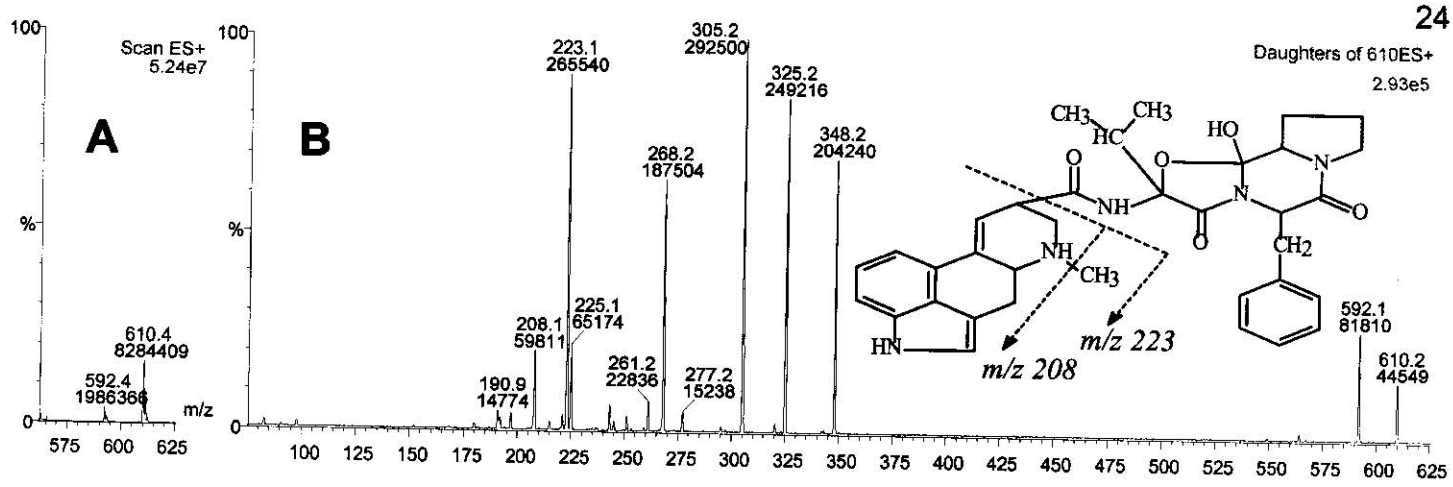

Fig. 7. Ergocrystine mass spectrometry. **A**, ESI(+) MS of ergocrystine standard infused as a 0.2 ug/ml solution in acetonitrile:0.05% formic acid at 1.0 ml/hr into the Quattro II MS. **B**, daughter ion spectrum of the m/z 610.4 fragment seen in **A**. Daughter ion principal peak assignments: m/z 610, $[M+H]^+$; 592, loss of water (-18) from peptide ring system; 564 [minor], 592 minus CO; 348, cleavage of peptide ring system (in amide and at ether); 325, m/z 592 minus [lysergic ring system-C=O-NH_2]; 305, m/z 592 minus R_2 group plus cleavage of lysergic D ring to retain first 2 carbons; 268, [lysergic ring system-C=O-NH_2] + H; 225, likely +H_2 variant of m/z 223; 223, $[M+H]^+$ minus [peptide side chain-NH_2-HC=O]; 208, m/z 223 minus CH_3; 197, m/z 223 minus CH≡CH; 180, 223 minus CH_2=NCH_3; 70, pyrrole ring + H; 44, CH_2=$NHCH_3$. The insert shows ergocrystine structure protonated on the lysergic ring tertiary amine and indicating collisionally-induced dissociation with the origins of the m/z 223 and 208 fragments.

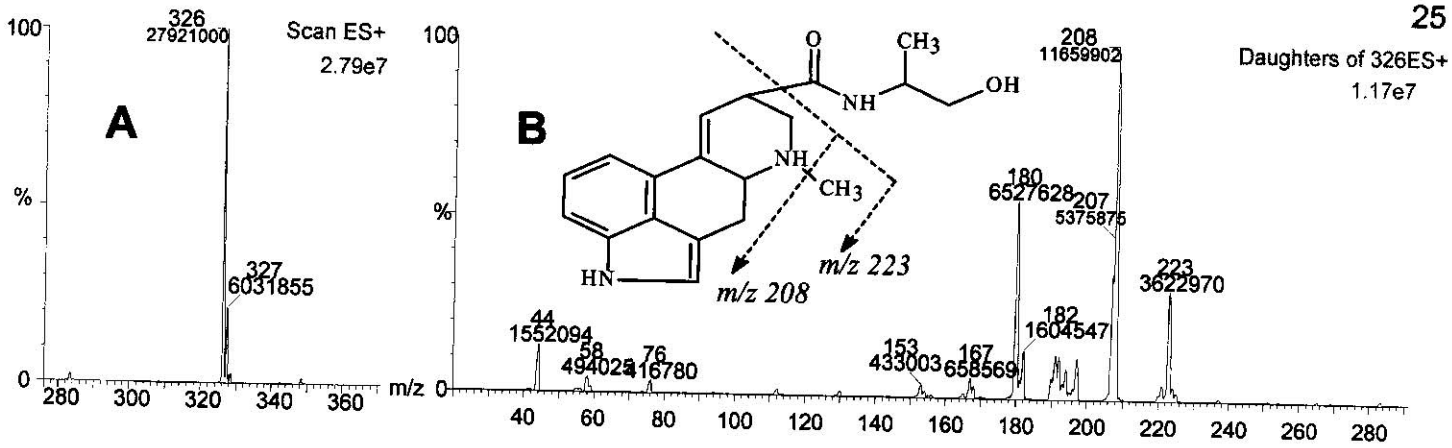

Fig. 8. Ergonovine mass spectrometry. **A**, ESI(+) MS of ergonovine infused as a 0.2 ug/ml solution in acetonitrile:0.05% formic acid at 1.0 ml/hr into the Quattro II MS. **B**, daughter ion spectrum of the m/z 326 fragment seen in **A**. Daughter ion principal peak assignments: m/z 223, loss of side chain [$H(C{=}O)NHCH(CH_3)CH_2OH$]; 208, m/z 223 minus CH_3; 197, m/z 223 minus $HC{\equiv}CH$; 180, m/z 223 minus $CH_2{=}NCH_3$; 167, m/z 223 minus $CH_2{=}CHNCH_3$; 76, $NH_3CH(CH_3)CH_2OH$ side chain; 44, $CH_2{=}NHCH_3$. The insert shows ergonovine structure protonated on the lysergic ring tertiary amine and indicating collisionally-induced dissociation with the origins of the m/z 223 and 208 fragments.

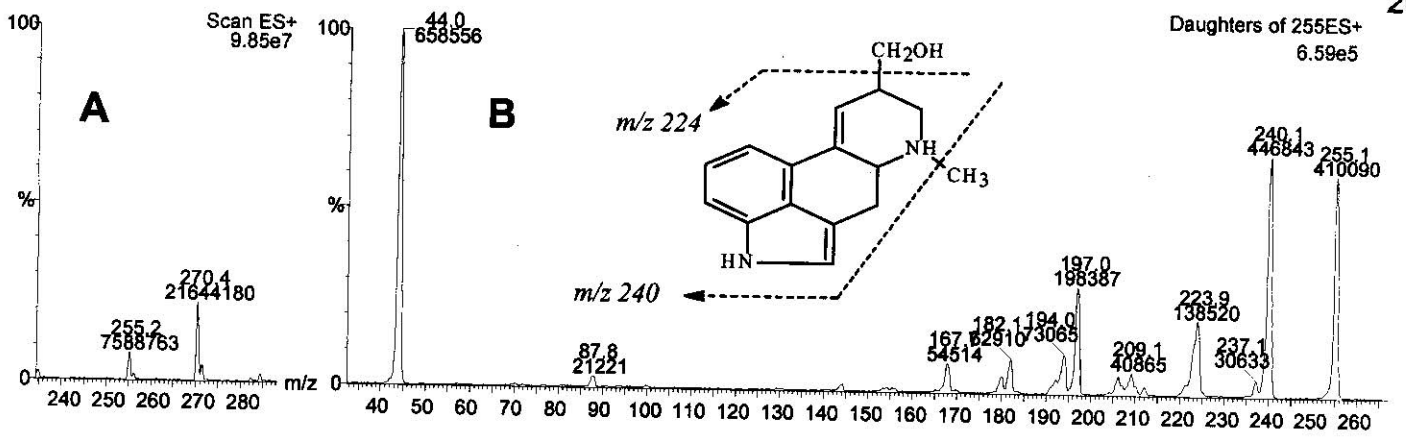

Fig. 9. Lysergol mass spectrometry.**A**, ESI(+) MS of lysergol standard infused as a 0.2 ug/ml solution in acetonitrile:0.05% formic acid at 1.0 ml/hr into the Quattro II MS. **B**, daughter ion spectrum of the m/z 255.1 fragment seen in **A**. More information on the m/z 270 fragment is presented in a later section. Daughter ion principal peak assignments: m/z 255, $[M+H]^+$; 240, $[M+H]^+$ minus CH_3; 224, $[M+H]^+$ minus CH_2OH; 209, m/z 240 minus CH_2OH; 197, $[M+H]^+$ minus $CH_2{=}CHCH_2OH$; 182, m/z 240 minus $CH_2{=}CHCH_2OH$; 168, $[M+H]^+$ minus $CH_3NCH_2{=}CH(CH)CH_2OH$; 88, $CH_3NHCH_2{=}CHCH_2OH$; 44, $CH_2{=}NHCH_3$. The insert shows lysergol structure protonated on the lysergic ring tertiary amine and indicating collisionally-induced dissociation with the origins of the m/z 224 and 240 fragments.

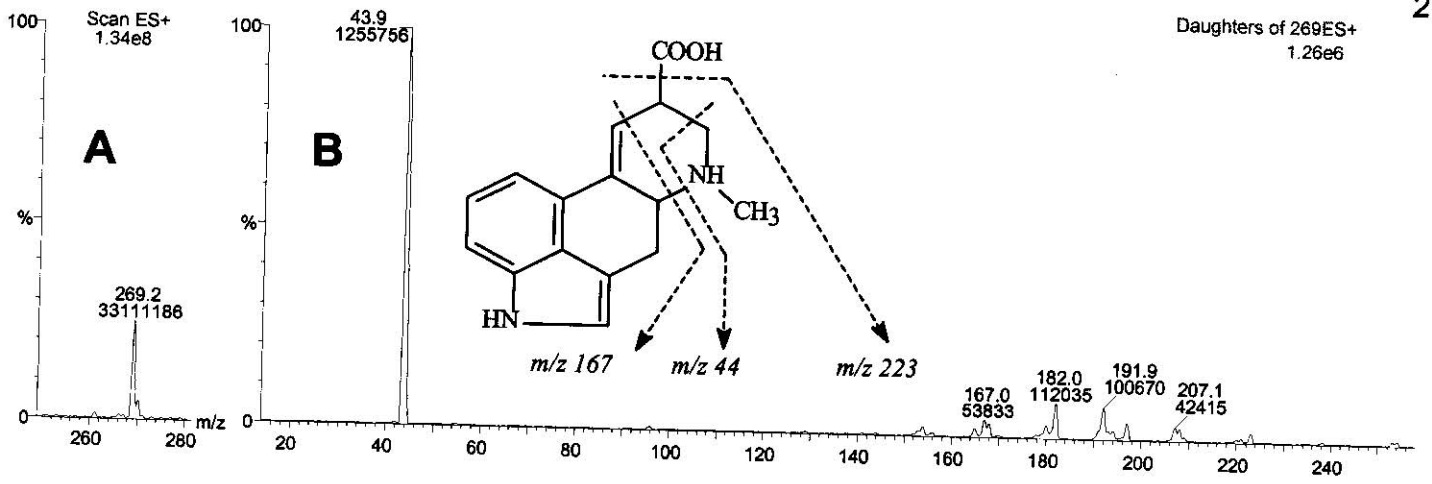

Fig. 10. Lysergic acid mass spectrometry. **A**, ESI(+) MS of lysergic acid standard infused as a 0.2 ug/ml solution in acetonitrile:0.05% formic acid at 1.0 ml/hr into the Quattro II MS. **B**, daughter ion spectrum of the m/z 269.1 fragment seen in **A**. Daughter ion principal peak assignments: m/z 254, $[M+H]^+$ minus CH_3; 223, $[M+H]^+$ minus HCOOH; 207, m/z 223 minus NH_2; 192, $[M+H]^+$ ring cleavage to release C_4H_3N=C; 182, m/z 254 minus CH_2=CHCOOH; 167, $[M+H]^+$ minus CH_3NHCH_2=CHCOOH; 44, CH_2=$NHCH_3$. The insert shows lysergic acid structure protonated on the lysergic ring tertiary amine and indicating collisionally-induced dissociation with the origins of the m/z 223, 167 and 44 fragments.

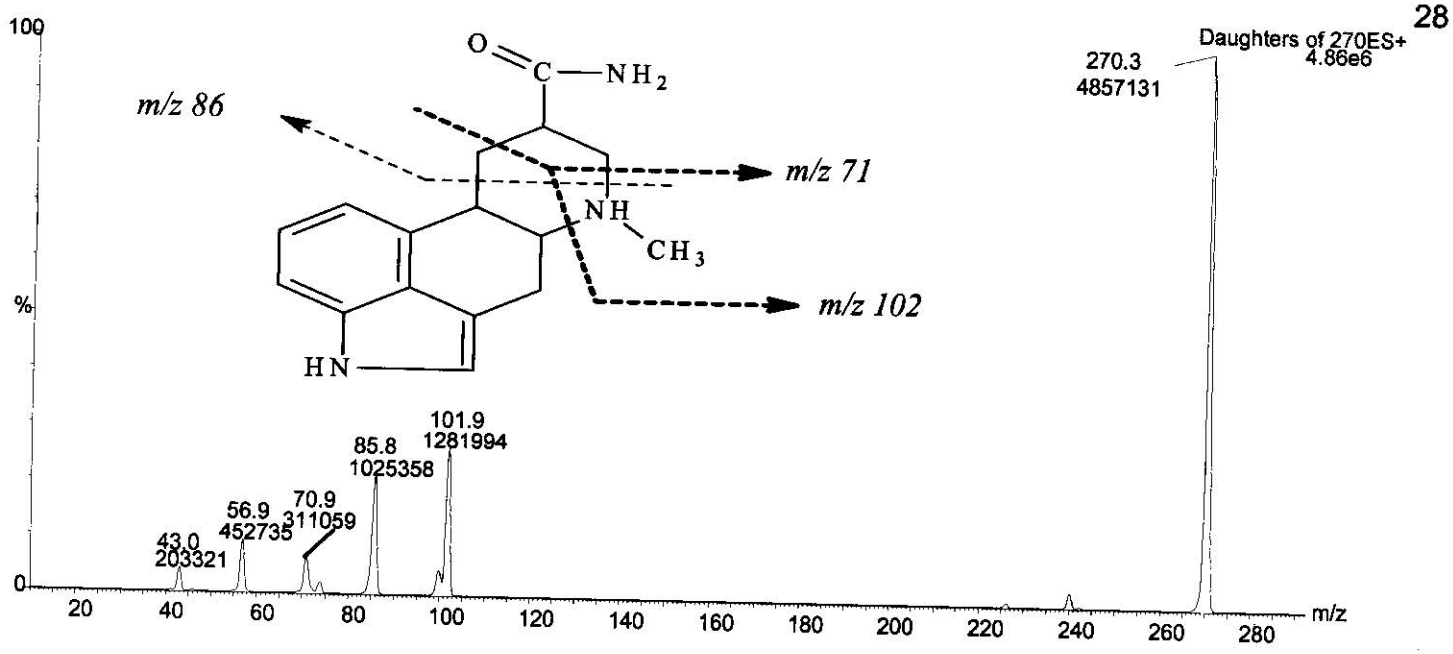

Fig. 11. Recurrent mass spectral m/z 270 fragment ($C_{16}H_{20}N_3O$) seen on scans of some ergot alkaloid preparations, e.g. ergovaline, ergocryptine, and lysergol, likely representing a common breakdown product or derivative. Seen at m/z 270, in this case during alpha-ergocryptine mass spectrometry with ESI(+) MS of alpha-ergocryptine infused as a 0.2 ug/ml solution in acetonitrile:0.05% formic acid at 1.0 ml/hr into the Quattro II MS. The spectrum represents m/z 270 daughter ions. Daughter ion principal peak assignments: m/z 270, $[M+H]^+$; 240, [M+H] minus CH_2NH_2; 102, $CH_3NH_2CH_2CHC(=O)NH_2$ or variant; 86, C_4H_8NO; 74, C_3H_8NO; 71, C_3H_5NO; 57, possible C_3H_5O fragment from m/z 102 for example; 43, $CH_3N=CH_2$. The insert shows one possible structure protonated on the lysergic ring tertiary amine and indicating collisionally-induced dissociation with the origins of the m/z 102, 86 and 71 fragments.

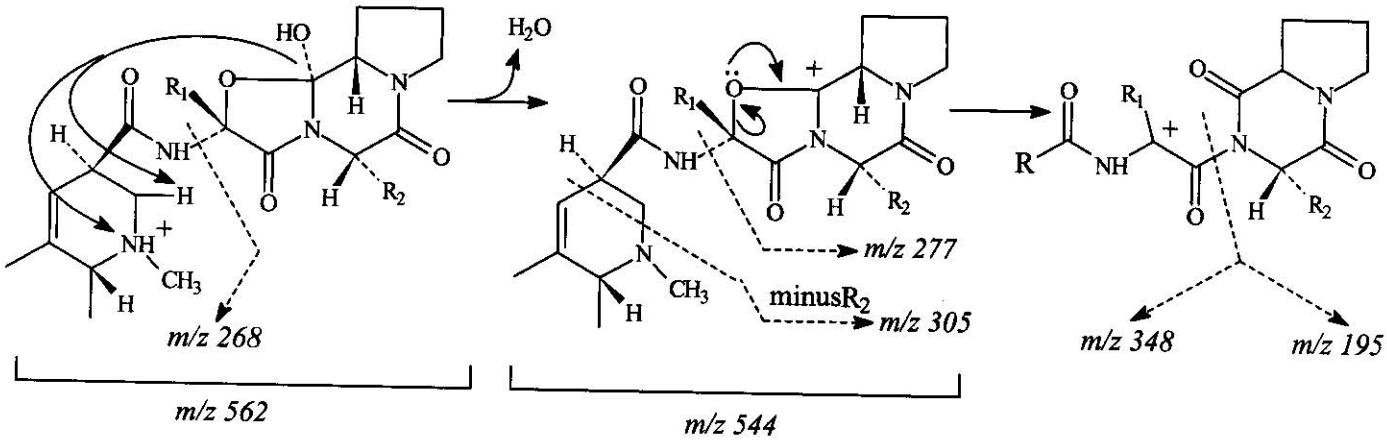

Fig. 12. Possible scheme for principal fragmentation mechanisms, in this case to account for principal peaks in ergocornine protonated on the lysergic ring tertiary amine as an example [R_1 = $CH_2(CH_3)_2$, R_2 = $CH_2(CH_3)_2$]. Protonation at the lysergic D-ring tertiary amine provides $[M+H]^+$ = m/z 562. Cleavage at the central amide releases the lysergic ring system as m/z 268; alternatively, dehydration at the tertiary alcohol via intramolecular proton extraction induces charge migration with generation of a tertiary carbonium ion, m/z 544; the dehydrate cleaves to release m/z 277 or m/z 305 [with release of R_2], or rearranges with migration of charge to provide an intermediate that cleaves to account for m/z 348 or the minor fragment m/z 195.

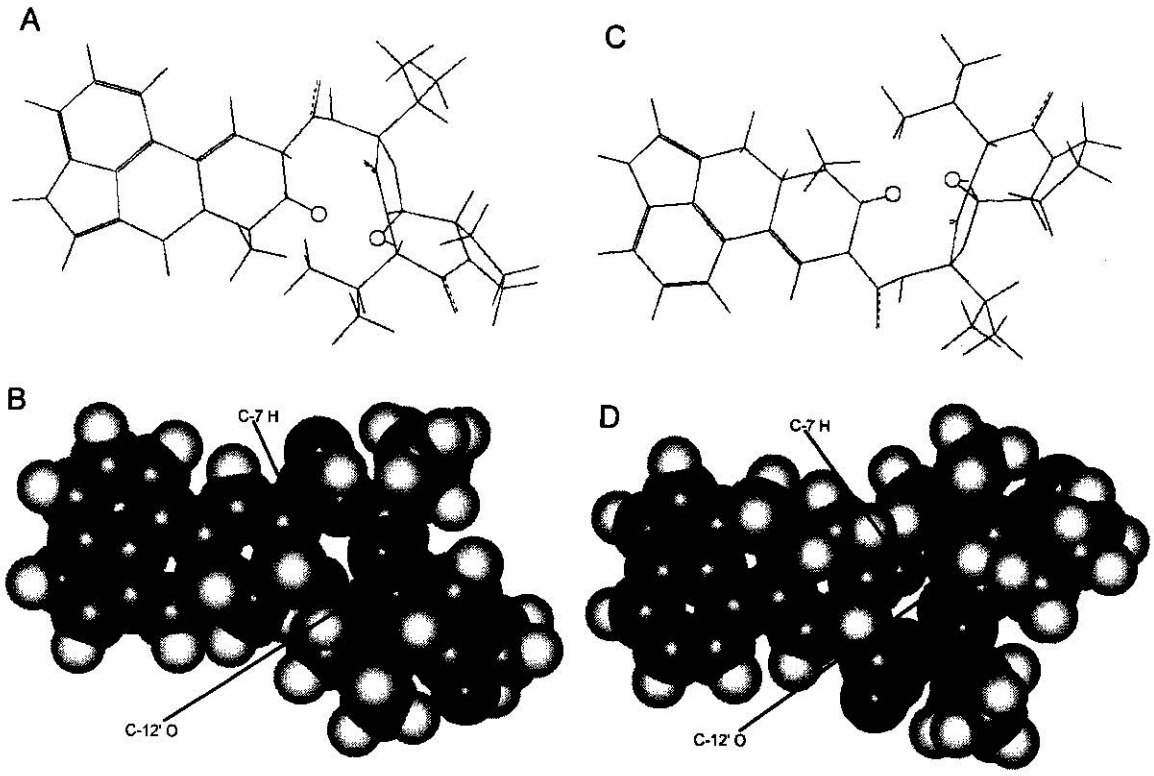

Figure 13. Demonstration of proximity of lysergic D and peptide F rings. Geometry-optimized structure of ergocornine provided by Hyperchem software. **A** and **B** show stick figure and space-filling views from the same side of the molecule, with the lysergic ring system to the left and oriented similarly to the graphical representation in Fig. 1. **C** and **D** show the same from the opposite side (rotation along a latitudinal axis). Circles in **A** and **C**, and arrows in **B** and **D** indicate the C-7 alpha proton (C-7 H) and the C-12' hydroxyl oxygen atom (C-12' O), which are separated by a calculated distance of only 1.831 Å.

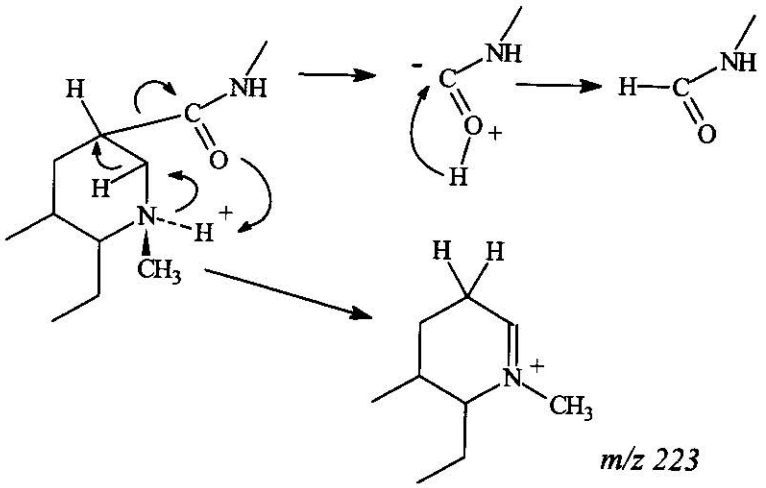

Fig. 14. Possible fragmentation pathway to the m/z 223 fragment seen in Figs. 2-3 and 5-8. Protonation of the lysergic ring system tertiary amine imparts a positive charge; intramolecular proton transfer to the central amide linkage carbonyl group results in a positively charged immonium group upon electron transfer. Subsequent or simultaneous cleavage to release the amide and adjacent protein group results in a leaving group with temporary charge separation that resolves by shift of a proton to give a neutral structure.

Tables

Table 1. Ion fragments common to ergot alkaloid standards; x = fragment found as a peak in compound's daughter ion mass spectrum. R_1 and R_2 substituents refers to Fig. 1.

m/z	1	2	3	4	5	6	7	8	assignment
R_1	me	me	ipr	ipr	ipr	(me)	-	-	
R_2	ipr	bzl	ipr	ibu	bzl	-	-	-	
[M+H] - 18	x	x	x	x	x				loss of water [peptide ring system tertiary alcohol]
[[M+H] - 18] - 28	x	x	x	x	x				loss of CO from dehydrate
[[M+H] - 18] - 267	x	x	x	x	x				loss of [lysergic ring-$CONH_2$] from dehydrate
[[M+H] - 18] - 224	x								loss of [lysergic ring] from dehydrate
348			x	x	x				cleavage within and loss of most of peptide ring system (in amide and at ether) to include isopropyl group
320	x	x							cleavage within and loss of most of peptide ring system (in amide and at ether) to include methyl group
305			x	x	x				loss of R_2 from dehydrate plus cleavage of lysergic D ring to retain first 2 carbons
291				x					loss of R_1 and lysergic ring system from dehydrate
277	x		x						loss of R_1 and lysergic ring system from dehydrate
268	x	x	x	x	x				[lysergic ring system-C=O-NH_2] + H
251	x	x	x	x	x				m/z 268 minus NH_3
225	x	x	x	x	x				peptide ring system released by cleavage of M+H central amide group, minus alkyl or aralkyl side groups
223	x	x	x	x	x	x		x	[M+H] minus [peptide side chain-NH_2-HC=O]
208	x	x	x	x	x	x		x	m/z 223 minus CH_3
197	x	x	x	x	x	x	x	x	m/z 223 minus CH≡CH
180	x	x	x	x	x	x	x	x	m/z 223 minus CH_2=NCH_3
167			x			x		x	m/z 223 minus CH_2=$CHNCH_3$
70	x	x	x	x	x				peptide ring system pyrrole [C_4H_8N]
44	x	x	x	x	x	x	x	x	CH_2=$NHCH_3$

1=ergovaline; 2=ergotamine; 3=ergocornine; 4=ergocryptine; 5=ergocrystine; 6=ergonovine; 7=lysergol; 8=lysergic acid; abbreviations: me=methyl, ipr=isopropyl, ibu=isobutyl, bzl=benzyl, x = fragment present.

Table 2. Predicted nominal M+H and daughter ions for ergot alkaloids.

Compound	m.w.	M+H, m/z	daughters, m/z
dihydroergocristine	611	612	225,210
ergocristine	609	610	223,208
ergostine	595	596	223,208
ergotamine	581	582	223,208
dihydroergocryptine	577	578	225,210
ergocryptine	575	576	223, 208
dihydroergocornine	563	564	225,210
ergotamine dehydrate	563	564	223,208
ergocornine	561	562	223,208
ergoptine	561	562	223,208
ergonine	547	548	223,208
ergosine	547	548	223,208
ergovaline	533	534	223,208
nicergoline	483	484	214,199
cabergoline	451	452	251,210
ergonovine	325	326	223,208